

# Nuclear energy density functionals for astrophysics: from BSk16 to BSk21

Nicolas Chamel

Institut d'Astronomie et d'Astrophysique  
Université Libre de Bruxelles, Belgique

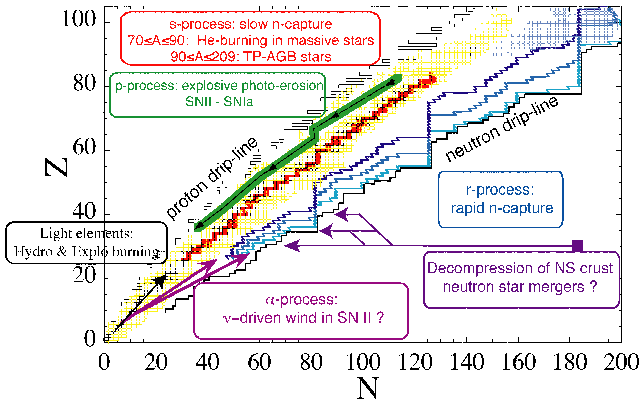


**ULB**



YIPQS, Kyoto, September 2011

The interpretation of many astrophysical phenomena requires the knowledge of nuclear properties which are not experimentally accessible



# Nuclear energy density functional theory in a nut shell

The nuclear energy density functional theory allows for a **tractable and consistent** treatment of various nuclear systems from atomic nuclei to neutron stars.

The energy of a lump of matter is expressed as ( $q = n, p$ )

$$E = \int \mathcal{E} \left[ \rho_q(\mathbf{r}), \nabla \rho_q(\mathbf{r}), \tau_q(\mathbf{r}), \mathbf{J}_q(\mathbf{r}), \tilde{\rho}_q(\mathbf{r}) \right] d^3\mathbf{r}$$

where  $\rho_q(\mathbf{r}), \tau_q(\mathbf{r}) \dots$  are functionals of  $\varphi_{1k}^{(q)}(\mathbf{r})$  and  $\varphi_{2k}^{(q)}(\mathbf{r})$

$$\begin{pmatrix} h_q(\mathbf{r}) - \lambda_q & \Delta_q(\mathbf{r}) \\ \Delta_q(\mathbf{r}) & -h_q(\mathbf{r}) + \lambda_q \end{pmatrix} \begin{pmatrix} \varphi_{1k}^{(q)}(\mathbf{r}) \\ \varphi_{2k}^{(q)}(\mathbf{r}) \end{pmatrix} = E_k^{(q)} \begin{pmatrix} \varphi_{1k}^{(q)}(\mathbf{r}) \\ \varphi_{2k}^{(q)}(\mathbf{r}) \end{pmatrix}$$

$$h_q \equiv -\nabla \cdot \frac{\delta E}{\delta \tau_q} \nabla + \frac{\delta E}{\delta \rho_q} - i \frac{\delta E}{\delta \mathbf{J}_q} \cdot \nabla \times \boldsymbol{\sigma}, \quad \Delta_q \equiv \frac{\delta E}{\delta \tilde{\rho}_q}$$

## Effective nuclear energy density functional

- In principle, one can construct the nuclear functional from realistic NN forces (i.e. fitted to experimental NN phase shifts) using many-body methods

$$\mathcal{E} = \frac{\hbar^2}{2M}(\tau_n + \tau_p) + A(\rho_n, \rho_p) + B(\rho_n, \rho_p)\tau_n + B(\rho_p, \rho_n)\tau_p$$

$$+ C(\rho_n, \rho_p)(\nabla \rho_n)^2 + C(\rho_p, \rho_n)(\nabla \rho_p)^2 + D(\rho_n, \rho_p)(\nabla \rho_n) \cdot (\nabla \rho_p)$$

+ Coulomb, spin-orbit and pairing

*Drut et al., Prog.Part.Nucl.Phys.64(2010)120.*

- But this is a very difficult task so in practice, we use phenomenological (generalized Skyrme) functionals  
*Bender et al., Rev.Mod.Phys.75, 121 (2003).*

## Phenomenological corrections for atomic nuclei

For atomic nuclei, we add the following corrections not taken into account in Skyrme functionals:

- Wigner energy

$$E_W = V_W \exp \left\{ -\lambda \left( \frac{N-Z}{A} \right)^2 \right\} + V'_W |N-Z| \exp \left\{ -\left( \frac{A}{A_0} \right)^2 \right\}$$

- rotational and vibrational spurious collective energy

$$E_{\text{coll}} = E_{\text{rot}}^{\text{crank}} \left\{ b \tanh(c|\beta_2|) + d|\beta_2| \exp\{-l(|\beta_2| - \beta_2^0)^2\} \right\}$$

In this way, these collective effects do not contaminate the parameters of the functional.

# Construction of the functional

## Experimental data:

- 2149 atomic masses with  $Z, N \geq 8$  from AME 2003
- compressibility  $230 \leq K_v \leq 250$  MeV
- charge radius of  $^{208}\text{Pb}$ ,  $R_c = 5.501 \pm 0.001$  fm
- symmetry energy  $J = 30$  MeV

## N-body calculations with realistic forces:

- isoscalar effective mass  $M_s^*/M = 0.8$
- equation of state of pure neutron matter
- $^1S_0$  pairing gaps in symmetric and neutron matter
- Landau parameters, stability against spurious spin and spin-isospin instabilities

With these constraints, the functional is well suited for astrophysical applications.

# Empirical pairing energy density functionals

The pairing functional is generally parametrized as

$$\mathcal{E}_{\text{pair}} = \frac{1}{4} \sum_{q=n,p} v^{\pi q}[\rho_n, \rho_p] \tilde{\rho}_q^2$$

$$v^{\pi q}[\rho_n, \rho_p] = V_{\pi q}^{\Lambda} \left( 1 - \eta_q \left( \frac{\rho_n + \rho_p}{\rho_0} \right)^{\alpha q} \right)$$

## Drawbacks

- not enough flexibility to fit realistic pairing gaps in infinite nuclear matter and in finite nuclei ( $\Rightarrow$  isospin dependence)
- the global fit to nuclear masses would be computationally very expensive

# Microscopically deduced pairing functional

## Assumptions:

- $v^{\pi q}[\rho_n, \rho_p] = v^{\pi q}[\rho_q]$  depends *only* on  $\rho_q$   
*Duguet, Phys. Rev. C 69 (2004) 054317.*
- isospin charge symmetry  $v^{\pi n} = v^{\pi p} = v^{\pi}$
- $v^{\pi}[\rho_q]$  is the *locally* the same as in infinite nuclear matter with density  $\rho_q$

$v^{\pi}[\rho_q] = v^{\pi}[\Delta_q(\rho_q)]$  constructed so as to reproduce *exactly* a given pairing gap  $\Delta_q(\rho_q)$  in infinite homogeneous matter by solving *directly* the HFB equations

*Chamel, Goriely, Pearson, Nucl. Phys.A812,72 (2008).*



## Pairing in nuclei and in nuclear matter

Inverting the HFB equations yields

$$v^\pi[\rho_q] = -8\pi^2 \left( \frac{\hbar^2}{2M_q^*} \right)^{3/2} \left( \int_0^{\mu_q + \varepsilon_\Lambda} d\varepsilon \frac{\sqrt{\varepsilon}}{\sqrt{(\varepsilon - \mu_q)^2 + \Delta_q(\rho_q)^2}} \right)^{-1}$$

$$\mu_q = \frac{\hbar^2}{2M_q^*} (3\pi^2 \rho_q)^{2/3}$$

Cutoff prescription: s.p. energy cutoff  $\varepsilon_\Lambda$  above the Fermi level

This procedure provides a one-to-one correspondence between the pairing strength in finite nuclei and the  $^1S_0$  pairing gap in infinite nuclear matter.

## Analytical expression of the pairing strength

In the “weak-coupling approximation”  $\Delta_q \ll \mu_q$  and  $\Delta_q \ll \varepsilon_\Lambda$

$$v^\pi[\rho_q] = -\frac{8\pi^2}{I_q(\rho_q)} \left( \frac{\hbar^2}{2M_q^*(\rho_q)} \right)^{3/2}$$

$$I_q = \sqrt{\mu_q} \left[ 2 \log \left( \frac{2\mu_q}{\Delta_q} \right) + \Lambda \left( \frac{\varepsilon_\Lambda}{\mu_q} \right) \right]$$

$$\Lambda(x) = \log(16x) + 2\sqrt{1+x} - 2 \log \left( 1 + \sqrt{1+x} \right) - 4$$

*Chamel, Phys. Rev. C 82, 014313 (2010)*

- **exact fit** of the given gap function  $\Delta_q(\rho_q)$
- **no free parameters**
- **automatic renormalization** of the pairing strength with  $\varepsilon_\Lambda$

## Pairing gaps from contact interactions

The weak-coupling approximation can also be used to determine the pairing gap of a Fermi gas interacting with a contact force

$$\Delta = 2\mu \exp\left(\frac{2}{g(\mu)v_{\text{reg}}^{\pi}}\right)$$

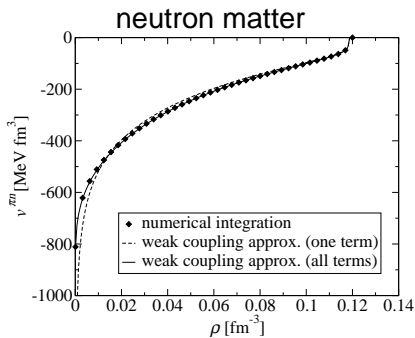
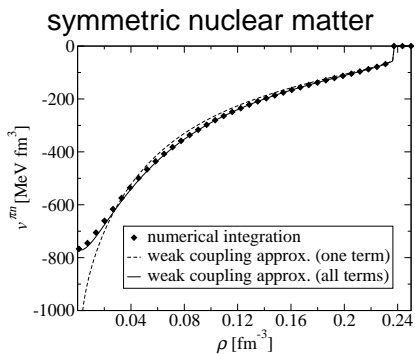
$\mu$  is the chemical potential,  $g(\mu)$  is the density of states and  $v_{\Lambda}^{\pi}$  is a regularized interaction

$$\frac{1}{v_{\text{reg}}^{\pi}} = \frac{1}{v^{\pi}} + \frac{1}{v_{\Lambda}^{\pi}}$$

$$v_{\Lambda}^{\pi} = \frac{4}{g(\mu)\Lambda(\varepsilon_{\Lambda}/\mu)}$$

## Accuracy of the weak-coupling approximation

This approximation remains very accurate at low densities because the s.p. density of states is not replaced by a constant as usually done.



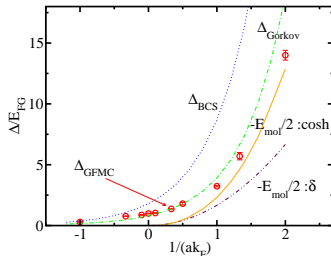
Chamel, *Phys. Rev. C* 82, 014313 (2010)

## Pairing in dilute neutron matter

At very low densities, the pairing gap is given by

$$\Delta_n = \left(\frac{2}{e}\right)^{7/3} \mu_n \exp\left(\frac{\pi}{2k_F a_{nn}}\right)$$

Gorkov&Melik-Barkhudarov, *Sov. Phys. JETP*, 13, 1018, (1961).



Chang et al. *Phys.Rev.A*70, 043602 (2004).

$$\Rightarrow v^\pi[\rho_n] = -\frac{8\pi^2}{I_n(\rho_n)} \left(\frac{\hbar^2}{2M_n^*(\rho_n)}\right)^{3/2}$$

$$I_n = \sqrt{\mu_n} \left[ \frac{14}{3} - \frac{8}{3} \log 2 - \left(\frac{\pi}{k_F a_{nn}}\right) + \Lambda \left(\frac{\varepsilon_\Lambda}{\mu_n}\right) \right]$$

## Pairing cutoff and experimental phase shifts

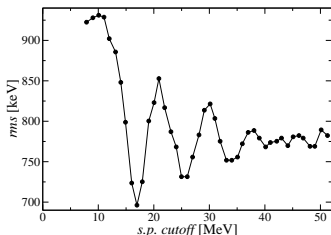
In the limit of vanishing density, the pairing strength

$$v^\pi[\rho_q \rightarrow 0] = -\frac{4\pi^2}{\sqrt{\varepsilon_\Lambda}} \left( \frac{\hbar^2}{2M_q} \right)^{3/2}$$

should coincide with the bare force in the  $^1S_0$  channel.

A fit to the **experimental  $^1S_0$  NN phase shifts** yields  
 $\varepsilon_\Lambda \sim 7 - 8$  MeV.

*Esbensen et al., Phys. Rev. C 56, 3054 (1997).*

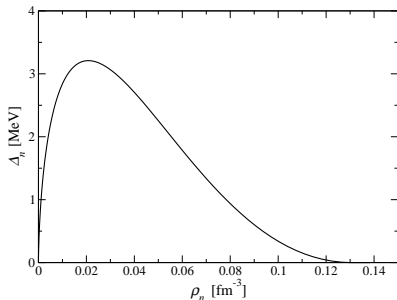


On the other hand, a better mass fit can be obtained with  $\varepsilon_\Lambda \sim 16$  MeV while convergence is achieved for  $\varepsilon_\Lambda \gtrsim 40$  MeV.

*Goriely et al., Nucl.Phys.A773(2006),279.*

## Choice of the pairing gap

Fit the  $^1S_0$  pairing gap obtained with realistic NN potentials at the BCS level



$^1S_0$  pairing gaps in neutron matter obtained with Argonne  $V_{14}$  potential

- $\Delta_n(\rho_n)$  essentially independent of the NN potential
- $\Delta_n(\rho_n)$  completely determined by experimental  $^1S_0$  nn phase shifts

*Dean&Hjorth-Jensen, Rev.Mod.Phys.75(2003)607.*

## Neutron vs proton pairing

- Because of possible **charge symmetry breaking effects**, proton and neutron pairing strengths may not be equal

$$v^{\pi n}[\rho] \neq v^{\pi p}[\rho]$$

- The neglect of **polarization effects in odd nuclei** (equal filling approximation) is corrected by “staggered” pairing

⇒ we introduce renormalization factors  $f_q^\pm$  ( $f_n^+ \equiv 1$  by definition)

$$v^{\pi n}[\rho_n] = f_n^\pm v^\pi[\rho_n]$$

$$v^{\pi p}[\rho_p] = f_p^\pm v^\pi[\rho_p]$$

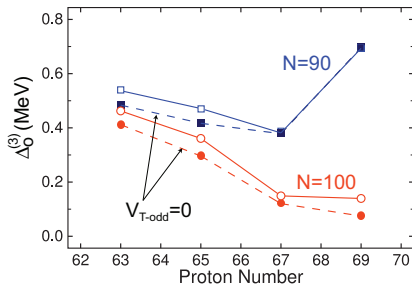


## Neutron vs proton pairing

What comes out of the global mass fit?

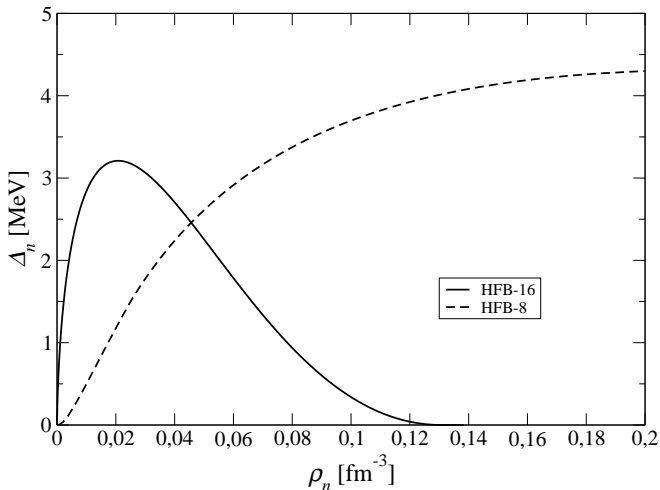
- neutron and proton pairing strengths are effectively equal  
 $f_n^- / f_n^+ \simeq f_p^- / f_p^+$
- the pairing strength is larger for odd than for even nuclei  
 $f_q^- \gtrsim f_q^+$

This is consistent with the analysis of Bertsch et al.  
*Phys.Rev.C79(2009),034306*



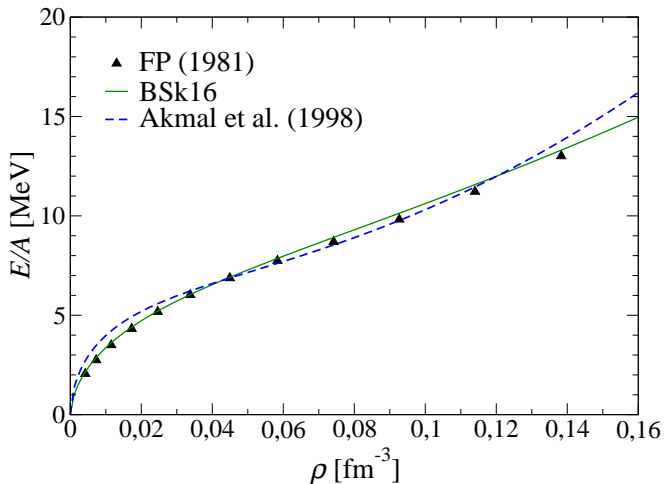
## $^1S_0$ pairing gap in neutron matter

This new mass model yields a much more realistic gap than our previous mass models!



## Neutron-matter equation of state

This mass model is in very good agreement with realistic neutron-matter equations of state



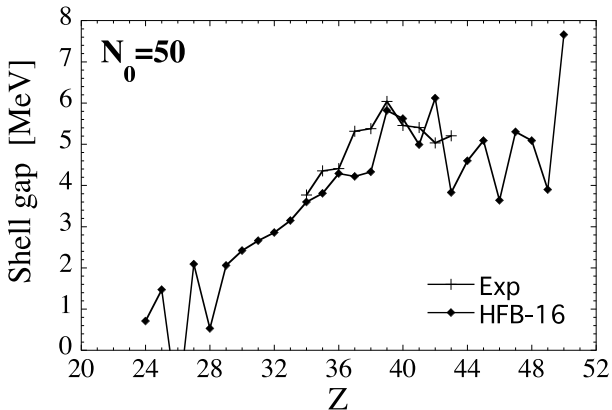
## HFB-16 mass table

Results of the fit on the 2149 measured masses with  $Z, N \geq 8$  from the 2003 Atomic Mass Evaluation

	HFB-16	FRDM
$\sigma(M)$ [MeV]	0.632	0.656
$\bar{\epsilon}(M)$ [MeV]	-0.001	0.058
$\sigma(M_{nr})$ [MeV]	0.748	0.919
$\bar{\epsilon}(M_{nr})$ [MeV]	0.161	0.047
$\sigma(S_n)$ [MeV]	0.500	0.399
$\bar{\epsilon}(S_n)$ [MeV]	-0.012	-0.001
$\sigma(Q_\beta)$ [MeV]	0.559	0.498
$\bar{\epsilon}(Q_\beta)$ [MeV]	0.031	0.004
$\sigma(R_C)$ [fm]	0.0313	0.0545
$\bar{\epsilon}(R_C)$ [fm]	-0.0149	-0.0366

## Pairing predictions in nuclei

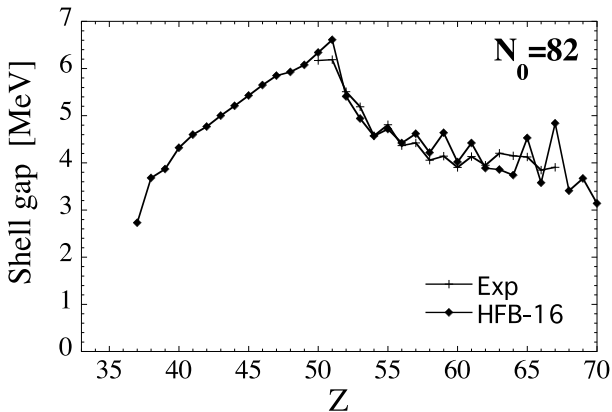
$N_0 = 50$  shell gap as function of  $Z$  for mass model HFB-16.



Chamel, Goriely, Pearson, *Nucl. Phys.A812,72 (2008)*

## Pairing predictions in nuclei

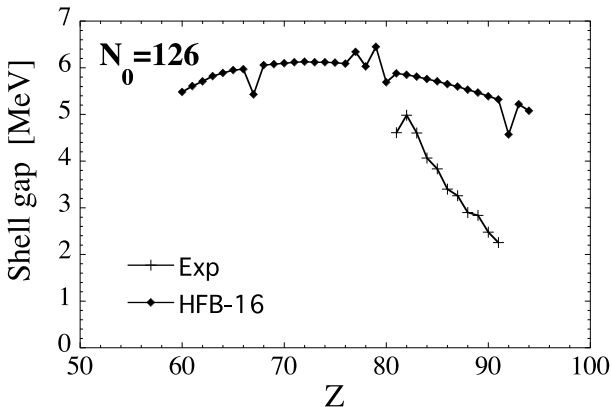
$N_0 = 82$  shell gap as function of  $Z$  for mass model HFB-16.



Chamel, Goriely, Pearson, *Nucl. Phys.A812,72 (2008)*

## Pairing predictions in nuclei

$N_0 = 126$  shell gap as function of  $Z$  for mass model HFB-16.

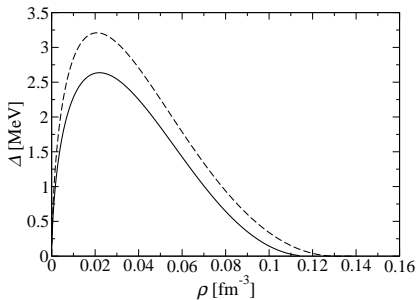


Chamel, Goriely, Pearson, *Nucl. Phys.A812,72 (2008)*

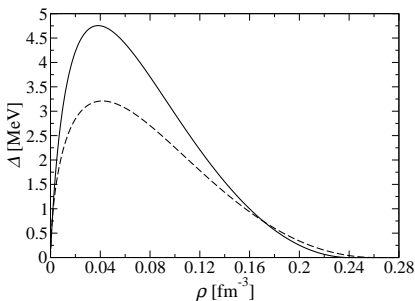
## HFB-17 mass model: microscopic pairing gaps including medium polarization effects

Fit the  $^1S_0$  pairing gaps of both neutron matter and symmetric nuclear matter obtained from **Brueckner calculations taking into account medium polarization effects**

Neutron matter



Symmetric nuclear matter



Cao et al., *Phys.Rev.C*74,064301(2006).



## New expression of the pairing strength

- the pairing strength is allowed to depend on both  $\rho_n$  and  $\rho_p$

$$v^{\pi q}[\rho_n, \rho_p] = v^{\pi q}[\Delta_q(\rho_n, \rho_p)]$$

- $\Delta_q(\rho_n, \rho_p)$  is interpolated between that of symmetric matter (SM) and pure neutron matter (NM)

$$\Delta_q(\rho_n, \rho_p) = \Delta_{SM}(\rho)(1 - |\eta|) \pm \Delta_{NM}(\rho_q) \eta \frac{\rho_q}{\rho}$$

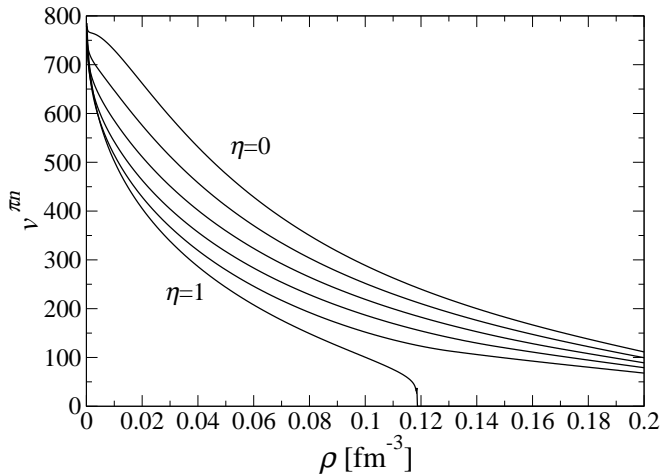
$$\eta = \frac{\rho_n - \rho_p}{\rho_n + \rho_p}$$

- $M_q^* = M$  to be consistent with the neglect of self-energy effects on the gap

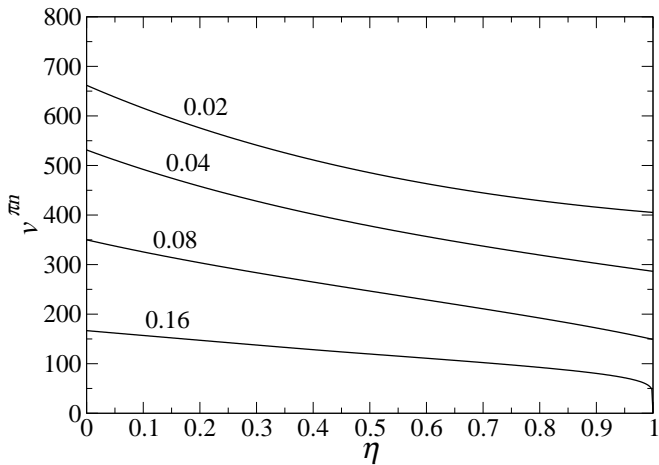
Goriely, Chamel, Pearson, *PRL* 102, 152503 (2009).

Goriely, Chamel, Pearson, *Eur.Phys.J.A* 42(2009), 547.

## Density dependence of the pairing strength



# Isospin dependence of the pairing strength



## HFB-17 mass table

Results of the fit on the 2149 measured masses with  $Z, N \geq 8$  from the 2003 Atomic Mass Evaluation

	HFB-16	HFB-17
$\sigma(2149 M)$	<b>0.632</b>	<b>0.581</b>
$\bar{\epsilon}(2149 M)$	-0.001	-0.019
$\sigma(M_{nr})$	0.748	0.729
$\bar{\epsilon}(M_{nr})$	0.161	0.119
$\sigma(S_n)$	0.500	0.506
$\bar{\epsilon}(S_n)$	-0.012	-0.010
$\sigma(Q_\beta)$	0.559	0.583
$\bar{\epsilon}(Q_\beta)$	0.031	0.022
$\sigma(R_c)$	0.0313	0.0300
$\bar{\epsilon}(R_c)$	-0.0149	-0.0114
$\theta(^{208}\text{Pb})$	0.15	0.15

## Predictions to newly measured atomic masses

HFB mass models were fitted to the 2003 Atomic Mass Evaluation.

**The predictions of these models are in good agreement with new mass measurements**

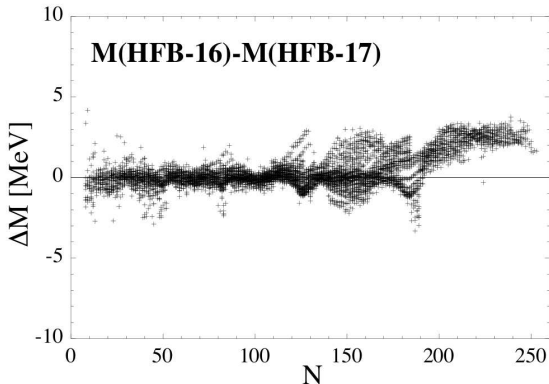
	HFB-16	HFB-17
$\sigma(434 M)$	0.484	0.363
$\bar{\epsilon}(434 M)$	-0.136	-0.092
$\sigma(142 M)$	0.516	0.548
$\bar{\epsilon}(142 M)$	-0.070	0.172

*Litvinov et al., Nucl.Phys.A756, 3(2005)*

[http://research.jyu.fi/igisol/JYFLTRAP\\_masses/gs\\_masses.txt](http://research.jyu.fi/igisol/JYFLTRAP_masses/gs_masses.txt)

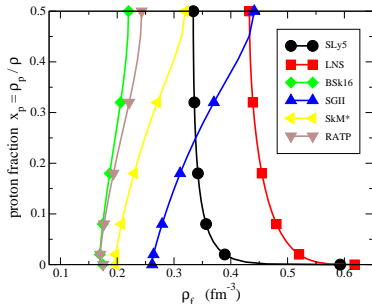
## Nuclear masses: HFB-16 vs HFB-17

Differences between the HFB-16 and HFB-17 mass predictions as a function  $N$  for all  $8 \leq Z \leq 110$  nuclei lying between the proton and neutron drip lines.

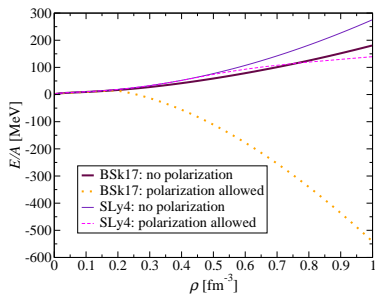


# Ferromagnetic instability

Unlike microscopic calculations, conventional Skyrme functionals predict a ferromagnetic transition in nuclear matter sometimes leading to a ferromagnetic collapse of neutron stars.



Margueron et al.,  
*J.Phys.G36(2009),125102.*



Chamel et al.,  
*Phys.Rev.C80(2009),065804.*

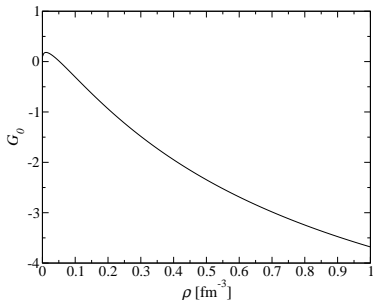
## Spin and spin-isospin instabilities

Skyrme functional in polarized homogeneous nuclear matter

$$\mathcal{E}_{\text{Sky}}^{\text{pol}} = \mathcal{E}_{\text{Sky}}^{\text{unpol}} + C_0^s \mathbf{s}^2 + C_1^s (\mathbf{s}_n - \mathbf{s}_p)^2 + C_0^T \mathbf{s} \cdot \mathbf{T} + C_1^T (\mathbf{s}_n - \mathbf{s}_p) \cdot (\mathbf{T}_n - \mathbf{T}_p)$$

with  $\mathbf{s}_q = \rho_{q\uparrow} - \rho_{q\downarrow}$  and  $\mathbf{T}_q = \tau_{q\uparrow} - \tau_{q\downarrow}$ .

Spurious spin and spin-isospin instabilities arise from the  $C_0^T$  and  $C_1^T$  terms in the Skyrme functional.



In symmetric nuclear matter, the ferromagnetic stability is governed by the Landau parameter  $G_0 = 2N_0(C_0^s + C_0^T k_F^2)$ .



## Spin stability in nuclear matter (partially) restored

The spurious ferromagnetic instability can be removed by including **spin density dependent** terms in the functional

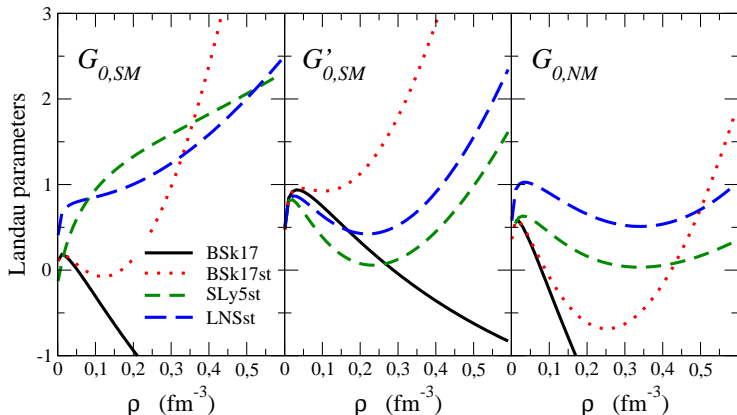
In the framework of effective Skyrme forces, this can be achieved by adding new terms of the form ( $\rho_s = S_n + S_p$ ,  
 $\rho_{st} = S_n - S_p$ )

$$\frac{1}{6} t_3^s (1 + x_3^s P_\sigma) \rho_s(\mathbf{r})^{\gamma_s} \delta(\mathbf{r}_{ij})$$
$$+ \frac{1}{6} t_3^{st} (1 + x_3^{st} P_\sigma) \rho_{st}(\mathbf{r})^{\gamma_{st}} \delta(\mathbf{r}_{ij})$$

*Margueron et al., J.Phys.G36(2009), 125102.*

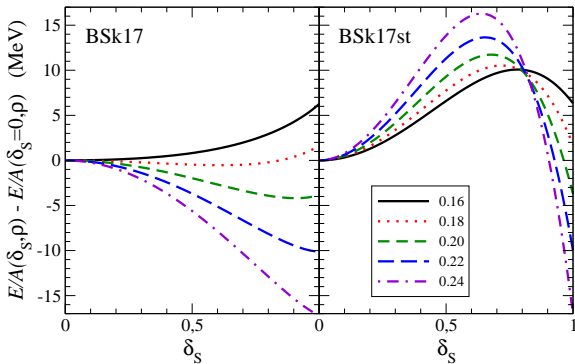
## Spin stability in nuclear matter (partially) restored

The spin-dependent terms not only remove the ferromagnetic instability but also slightly improve the mass fit ( $\sigma = 0.575$  MeV)



## Ferromagnetic transition at finite polarization

Problem: the new term removes the instability around  $\delta_S \equiv (\rho^\uparrow - \rho^\downarrow)/\rho = 0$  but still predicts a ferromagnetic transition at finite  $|\delta_S| > 0$



## Spin stability in symmetric nuclear matter restored

The ferromagnetic instability can be completely removed by including the **density-dependent** term in the Skyrme force

$$t_5(1 + x_5 P_\sigma) \frac{1}{\hbar^2} \mathbf{p}_{ij} \cdot \rho(\mathbf{r})^\beta \delta(\mathbf{r}_{ij}) \mathbf{p}_{ij}$$

Problem: this new term will also change the nuclear properties at low densities! Introduce another force of the form

$$\frac{1}{2} t_4(1 + x_4 P_\sigma) \frac{1}{\hbar^2} \left\{ \mathbf{p}_{ij}^2 \rho(\mathbf{r})^\beta \delta(\mathbf{r}_{ij}) + \delta(\mathbf{r}_{ij}) \rho(\mathbf{r})^\beta \mathbf{p}_{ij}^2 \right\}$$

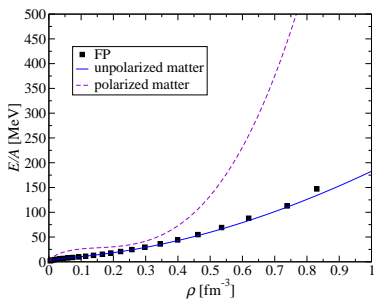
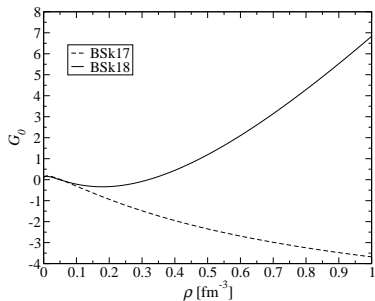
The  $t_4$  and  $t_5$  terms exactly cancel in unpolarized nuclear matter (for any isospin asymmetry) provided

$$t_4(1 - x_4) = -3t_5(1 + x_5), \quad x_4(5 + 4x_5) = -(4 + 5x_5)$$

*Chamel, Goriely, Pearson, Phys.Rev.C80(2009),065804.*

# Spin stability in asymmetric nuclear matter restored

With  $t_4$  and  $t_5$  terms, the ferromagnetic instability is completely removed not only in symmetric nuclear matter but also in neutron matter for any spin polarization.



We have checked that no instabilities arise in neutron stars at any densities.

*Chamel, Goriely, Pearson, Phys.Rev.C80(2009),065804.*

## HFB-18 mass model

Results of the fit on the 2149 measured masses with  $Z, N \geq 8$

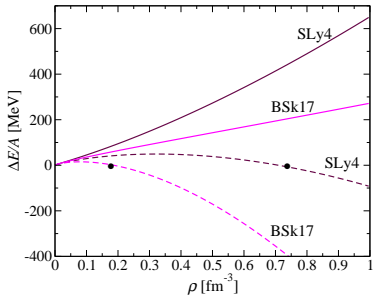
	HFB-18	HFB-17
$\sigma(M)$ [MeV]	0.585	0.581
$\bar{\epsilon}(M)$ [MeV]	0.007	-0.019
$\sigma(M_{nr})$ [MeV]	0.758	0.729
$\bar{\epsilon}(M_{nr})$ [MeV]	0.172	0.119
$\sigma(S_n)$ [MeV]	0.487	0.506
$\bar{\epsilon}(S_n)$ [MeV]	-0.012	-0.010
$\sigma(Q_\beta)$ [MeV]	0.561	0.583
$\bar{\epsilon}(Q_\beta)$ [MeV]	0.025	0.022
$\sigma(R_C)$ [fm]	0.0274	0.0300
$\bar{\epsilon}(R_C)$ [fm]	0.0016	-0.0114
$\theta(^{208}\text{Pb})$ [fm]	0.15	0.15

⇒ HFB-18 yields almost identical results as HFB-17 for nuclei

## Spin-isospin instabilities

Although HFB-18 yields stable neutron-star matter, it still predicts spurious spin-isospin instabilities in symmetric matter.

All instabilities (at any temperature and degree of polarization) can be removed by setting  $C_t^T = 0$ , which means dropping  $J^2$  terms due to gauge invariance.



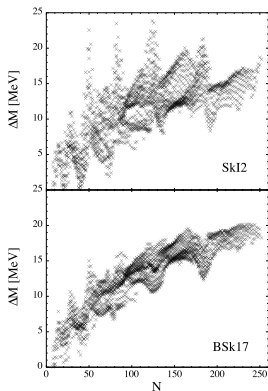
Difference between the energy per particle in fully polarized neutron matter and in unpolarized neutron matter with (dashed line) and without (solid line)  $C_t^T$  terms.

*Chamel&Goriely, Phys.Rev.C82, 045804 (2010)*

## Impact of the $J^2$ terms

Dropping the  $J^2$  terms and their associated time-odd parts

- removes spin and spin-isospin instabilities at any  $T \geq 0$
- prevents an anomalous behavior of the entropy
- improves the values of Landau parameters (especially  $G'_0$ ) and the sum rules.



### Warning:

Adding or removing a posteriori the  $J^2$  terms without refitting the functional can induce large errors!

*Chamel & Goriely, Phys.Rev.C82, 045804 (2010)*



## Landau parameters and the $J^2$ terms

Landau parameters for selected Skyrme forces which were fitted without the  $J^2$  terms. Values in parenthesis were obtained by setting  $C_t^T = 0$ .

	$G_0$	$G'_0$	$G_0^{\text{NeuM}}$
SGII	0.01 (0.62)	0.51 (0.93)	-0.07 (1.19)
SLy4	1.11 (1.39)	-0.13 (0.90)	0.11 (1.27)
SkI1	-8.74 (1.09)	3.17 (0.90)	-5.57 (1.10)
SkI2	-1.18 (1.35)	0.77 (0.90)	-1.08 (1.24)
SkI3	0.57 (1.90)	0.20 (0.85)	-0.19 (1.35)
SkI4	-2.81 (1.77)	1.38 (0.88)	-2.03 (1.40)
SkI5	0.28 (1.79)	0.30 (0.85)	-0.31 (1.30)
SkO	-4.08 (0.48)	1.61 (0.98)	-3.17 (0.97)
LNS	0.83 (0.32)	0.14 (0.92)	0.59 (0.91)
Microscopic	0.83	1.22	0.77

## Landau sum rules and the $J^2$ terms

Landau parameters must obey the sum rules

$$S_1 \equiv \sum_{\ell} \frac{F_{\ell}}{1 + F_{\ell}/(2\ell + 1)} + \frac{F'_{\ell}}{1 + F'_{\ell}/(2\ell + 1)} \\ + \frac{G_{\ell}}{1 + G_{\ell}/(2\ell + 1)} + \frac{G'_{\ell}}{1 + G'_{\ell}/(2\ell + 1)} = 0$$

$$S_2 \equiv \sum_{\ell} \frac{F_{\ell}}{1 + F_{\ell}/(2\ell + 1)} - 3 \frac{F'_{\ell}}{1 + F'_{\ell}/(2\ell + 1)} \\ - 3 \frac{G_{\ell}}{1 + G_{\ell}/(2\ell + 1)} + 9 \frac{G'_{\ell}}{1 + G'_{\ell}/(2\ell + 1)} = 0$$

## Landau sum rules and the $J^2$ terms

Landau sum rules for selected Skyrme forces which were fitted without the  $J^2$  terms. Values in parenthesis were obtained by setting  $C_t^T = 0$ .

	$S_1$	$S_2$
SGII	0.97 (0.61)	1.13 (-0.51)
SLy4	-0.31 (-0.65)	1.52 (0.85)
SkI1	-6.71 (-0.59)	-89.2 (0.86)
SkI2	6.87 (-0.71)	-20.7 (0.98)
SkI3	-1.46 (-2.33)	2.14 (1.84)
SkI4	1.01 (-1.23)	-11.3 (1.32)
SkI5	-1.47 (-2.28)	2.17 (1.77)
SkO	3.21 (1.07)	-13.7 (0.87)
LNS	0.49 (0.63)	3.53 (-0.04)

## More about the $J^2$ terms

On the other hand dropping the  $J^2$  terms leads to

- unrealistic effective masses in polarized matter

$$\frac{\hbar^2}{2M_{q\sigma}^*} = \frac{\hbar^2}{2M_q^*} \pm \left[ s(C_0^T - C_1^T) + 2s_q C_1^T \right] \Rightarrow M_{q\uparrow}^* = M_{q\downarrow}^* = M_q^*$$

- self-interaction errors.

Instabilities can be removed *with* the  $J^2$  terms by adding density-dependent terms in  $C_0^T$  and  $C_1^T$ . But only for  $T = 0$ .  
*Chamel, Goriely, Pearson, Phys.Rev.C80(2009),065804.*

## Self-interactions

In the one-particle limit, the potential energy obtained from phenomenological functionals may not vanish.

Considering the most general semi-local functional with all possible bilinear terms up to 2nd order in the derivatives

$$\begin{aligned}\mathcal{E}_{\text{Sky}} = & \sum_{t=0,1} C_t^\rho \rho_t^2 + C_t^{\Delta\rho} \rho_t \Delta\rho_t + C_t^T \rho_t \tau_t + C_t^{\nabla J} \rho_t \nabla \cdot \mathbf{J}_t \\ & + C_t^J \sum_{\mu,\nu} J_{t,\mu\nu} J_{t,\mu\nu} + \frac{1}{2} C_t^{TrJ} \left( \sum_{\mu} J_{t,\mu\mu} \right)^2 + \frac{1}{2} C_t^{J^2} \sum_{\mu,\nu} J_{t,\mu\nu} J_{t,\nu\mu} \\ & + C_t^s s_t^2 + C_t^{\Delta s} \mathbf{s}_t \cdot \Delta \mathbf{s}_t + C_t^T \mathbf{s}_t \cdot \mathbf{T}_t + C_t^{j_t^2} + C_t^{\nabla j} \mathbf{s}_t \cdot \nabla \times \mathbf{j}_t \\ & + C_t^{\nabla s} (\nabla \cdot \mathbf{s}_t)^2 + C_t^F \mathbf{s}_t \cdot \mathbf{F}_t\end{aligned}$$

## Removal of self-interactions

Requiring the cancellation of self-interactions leads to the fundamental constraints

$$C_0^\rho + C_1^\rho + C_0^s + C_1^s = 0$$

$$C_0^\tau + C_1^\tau + C_0^T + C_1^T = 4(C_0^{\Delta\rho} + C_1^{\Delta\rho} + C_0^{\Delta s} + C_1^{\Delta s})$$

$$4(C_0^{\nabla s} + C_1^{\nabla s}) + C_0^F + C_1^F = 0$$

$$C_0^\tau + C_1^\tau - 2(C_0^T + C_1^T) - (C_0^F + C_1^F) - 4(C_0^{\Delta s} + C_1^{\Delta s}) = 0$$

*Chamel, Phys. Rev. C 82, 061307(R) (2010).*

## Self-interaction errors

Self-interaction errors in the one-particle limit can contaminate systems consisting of many particles.

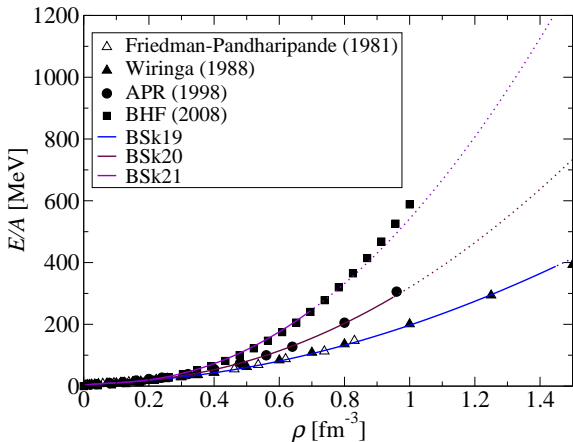
For instance, in polarized neutron matter the error in the energy density caused by self-interactions is given by

$$\delta\mathcal{E}_{\text{NeuM}}^{\text{pol}} = (C_0^\rho + C_1^\rho + C_0^s + C_1^s)\rho^2$$

If  $C_0^\rho + C_1^\rho + C_0^s + C_1^s < 0$ , self-interactions would thus drive a ferromagnetic collapse of neutron stars.

## Neutron-matter equation of state at high densities

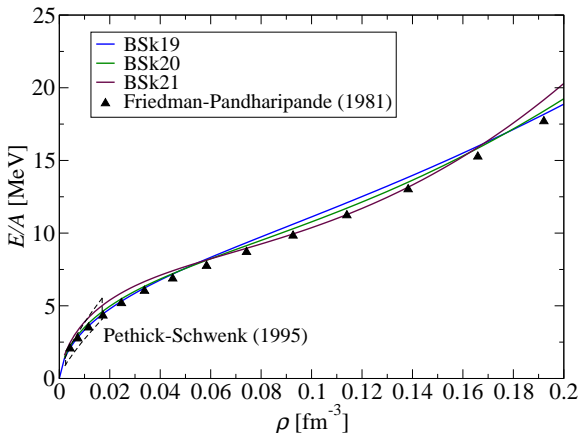
We have recently constructed a family of three different generalized Skyrme functionals BSk19, BSk20 and BSk21 spanning the range of realistic neutron-matter equations of state at high densities.





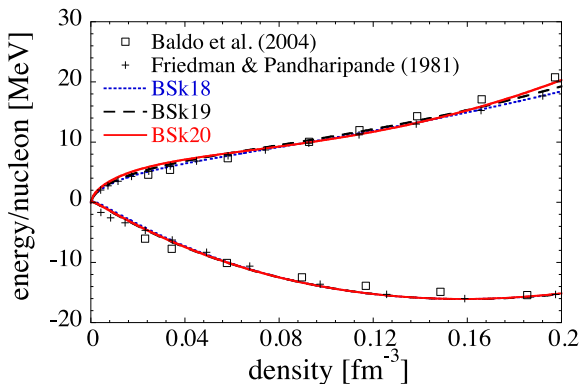
## Neutron-matter equation of state at low densities

All three functionals yield similar neutron-matter equations of state at subsaturation densities consistent with microscopic calculations using realistic NN interactions



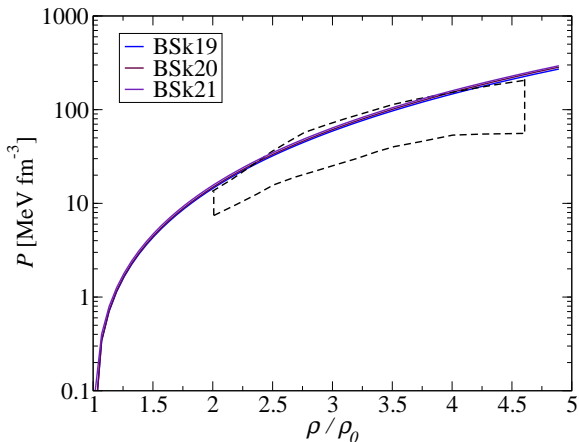
## Nuclear-matter equation of state

Our functionals are in very good agreement with BHF calculations not only in neutron matter but also in symmetric nuclear matter.



## Constraints from heavy-ion collisions

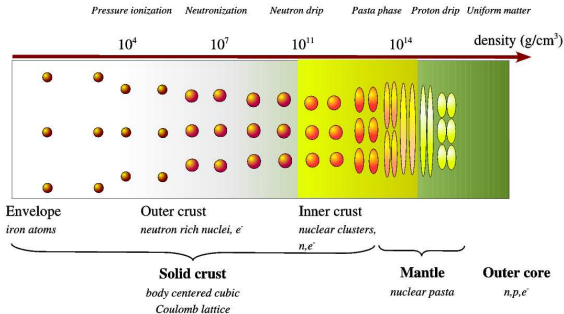
Our functionals are consistent with the pressure of symmetric nuclear matter inferred from Au+Au collisions



*Danielewicz et al., Science 298, 1592 (2002).*

# Internal constitution of neutron stars

The interior of a neutron star contains **very different phases of matter**. A unified description of all regions of neutron stars is therefore very challenging.



Chamel&Haensel, *Living Reviews in Relativity* 11 (2008), 10  
<http://relativity.livingreviews.org/Articles/lrr-2008-10/>

## Description of the outer crust of a neutron star

The interior of a neutron star is supposed to be made of “**cold catalyzed matter at the end point of thermonuclear evolution**”. *Harrison, Thorne, Wakano, Wheeler (1965)*

For each pressure  $P$ , minimize the Gibbs free energy per nucleon  $g = (\varepsilon + P)/n$  assuming a **perfect crystal of fully ionized atoms**

$$\varepsilon = n_I M\{A, Z\} + \varepsilon_e + \varepsilon_L$$

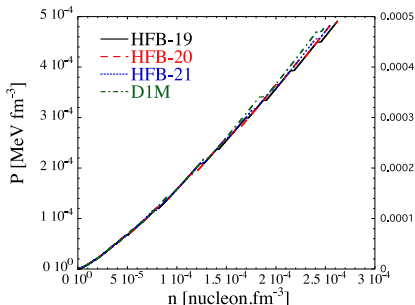
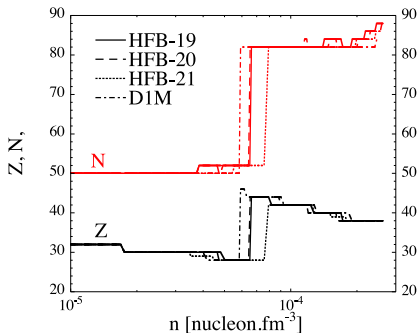
$M\{A, Z\}$  is the mass of an ion (atomic nucleus)

$\varepsilon_e$  is the energy density of the electron gas

$\varepsilon_L$  is the lattice energy density

# Ground-state composition of the outer crust of a cold non-accreting neutron star

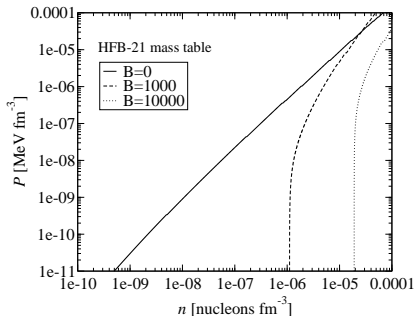
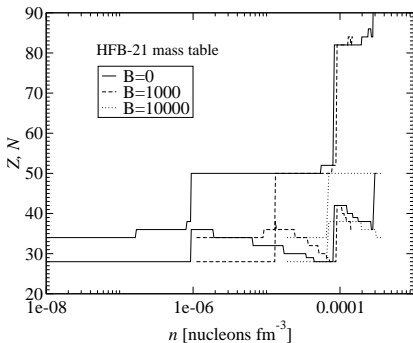
Nuclear masses are the only microscopic input.



*Pearson, Goriely and Chamel, Phys.Rev.C 83,065810(2011).*

# Ground-state composition of the outer crust of a strongly magnetized neutron star

In a strong magnetic field, the **electron motion perpendicular to the field is quantized** into Landau levels.



*Chamel, Pavlov, Mihailov, Velchev, Stoyanov, Mutafchieva (2011)*

## Description of neutron star crust beyond neutron drip

The equilibrium structure of the inner crust is determined with the Extended Thomas-Fermi (up to 4th order)+Strutinsky Integral method (ETFSI).

- Pairing is expected to have a small impact on the composition and is therefore neglected.
- Nuclei are assumed to be spherical.

*Onsi et al., Phys.Rev.C77,065805 (2008).*

### Advantages of ETFSI method

- very fast approximation to the full Hartree-Fock method
- avoids the difficulties related to boundary conditions but include proton shell effects (neutron shell effects are generally much smaller and can be omitted)

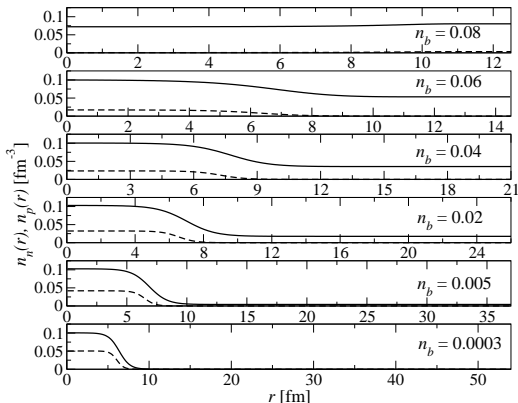
*Chamel et al., Phys.Rev.C75(2007),055806.*



# Ground-state composition of the inner crust

Results for BSk14

$n_b$ ( $\text{fm}^{-3}$ )	Z	A
0.0003	50	200
0.001	50	460
0.005	50	1140
0.01	40	1215
0.02	40	1485
0.03	40	1590
0.04	40	1610
0.05	20	800
0.06	20	780

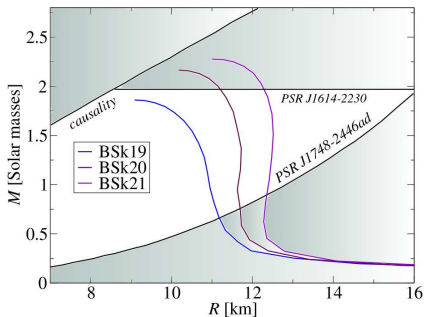
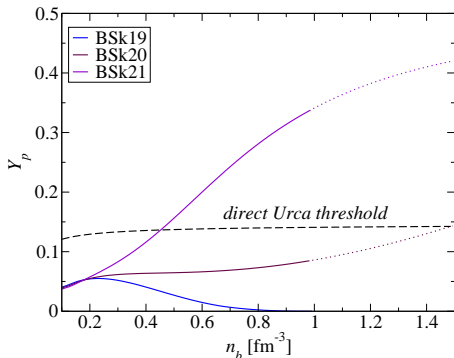


*Onsi, Dutta, Chatri, Goriely, Chamel and Pearson,  
Phys.Rev.C77,065805 (2008).*

With BSk19, BSk20 and BSk21, only  $Z = 40$  is found.

# Unified equation of state of neutron stars

All regions of neutron stars can be described using the same functional ( $n$ ,  $p$ ,  $e$ ,  $\mu$  matter in the core).



	$n_{caus}$ ( $\text{fm}^{-3}$ )	$\mathcal{M}_{max}/\mathcal{M}_{\odot}$	$R$ (km)	$n_{max}$ ( $\text{fm}^{-3}$ )
BSk19	1.45	1.86 (1.84)	9.13	1.45
BSk20	0.98	2.14 (2.20)	10.6	0.98
BSk21	0.99	2.28 (2.3)	11.0	0.97